GROUND DEFORMATION ANALYSIS USING BASIC PRODUCTS OF THE COPERNICUS GROUND MOTION SERVICE

S. Shahbazi [1*], M. Crosetto [1], A. Barra[1]

[1] Centre Tecnològic de Telecomunicacions de Catalunya (CTTC/CERCA), Geomatics Research Unit, Av. Gauss, 7, E-08860 Castelldefels (Barcelona), Spain. sshahbazi@cttc.es, mcrosetto@cttc.cat, abarra@cttc.cat

KEY WORDS: Copernicus, European Ground Motion Service, Gradient Deformation.

ABSTRACT:

Monitoring ground deformation at national and regional level with millimetre-scale precision, nowadays, is possible by using Advanced Differential Interferometric SAR (A-DInSAR) techniques. This study concerns the results of the European Ground Motion Service (EGMS), part of the Copernicus Land Monitoring Service, which detects and measures land displacement at European scale. This Service provides reliable and consistent information regarding natural ground motion phenomena such as landslides and subsidence. The ground motion is derived from Synthetic Aperture Radar (SAR) time-series analysis of Sentinel-1A/B data. These data, which provide full coverage of Europe from two different observation geometries (ascending and descending) every six days, are processed at full resolution. The paper is focused on the exploitation of the basic product of EGMS for both regional and local purposes. Analysing the slope and aspect of the deformation field is the novelty of this investigation. In particular, the focus is put on the generation of wide-area differential deformation maps. Such maps indicate the gradient of the deformation field. The obtained information is not only beneficial for monitoring anthropogenic phenomena but also vital for urban management and planning. Most of the significant damages to manmade structures and infrastructures are associated with high deformation gradient values. Thus, monitoring the temporal and spatial variations of deformation gradient is essential for dynamic analysis, early-warning, and risk assessment in urban areas. Although EGMS productions are prepared for monitoring at regional level, their resolutions are high enough to investigate at local level. Therefore, this paper considers the local deformations that affect single structures or infrastructures. Local differences in such deformation can indicate damages in the corresponding structures and infrastructures. We illustrate these types of analysis to generate differential deformation maps using datasets available at CTTC.

1. INTRODUCTION

Differential Interferometric SAR (DInSAR) is a powerful tool to detect and track ground movements. This technique is used in a wide range of research areas, like topography, ground surface deformation mapping, critical infrastructure monitoring, and others. During the previous two decades, the DInSAR and Persistent Scatterer Interferometry (PSI) approaches have advanced significantly. Furthermore, improvements of the A-DInSAR data processing and analysis techniques, besides increasing the computation capacity, result in monitoring capabilities over wide areas in sub-centimetre precision (Crosetto et al., 2016), (Ferretti et al., 2000), (Ferretti et al., 2001).

One of the key factors of using A-DInSAR is the availability of satellite-based SAR data. In this study we consider the European Commission's Sentinel-1 constellation, part of the Copernicus Programme, which includes two operational SAR sensors: Sentinel-1A and Sentinel-1B.

Sentinel-1 provides a global coverage and short revisiting time. Nowadays Sentinel-1 makes possible to monitor ground deformation over entire continents with a temporal resolution of 6 days, a spatial resolution of 14 by 14 m, with open data policy (Costantini et al., 2021).

The Copernicus European Ground Motion Service (EGMS) will process all Sentinel-1 data over most of Europe (Copernicus Participating States); it is implemented by the European Environment Agency (EEA). EGMS will employ persistent scatterer (PS) and distributed scatterer (DS) of InSAR processing techniques by using all acquisitions, both ascending and descending. The EGMS will a challenging application of A-DInSAR, to perform ground deformation monitoring over an entire continent in a harmonized form. Following the Copernicus data policy, the products of EGMS will be free and open. The service will provide tools for the visualization, the interactive data exploration, and the preliminary analysis of the products. (Crosetto et al., 2020a), (Crosetto et al., 2020b), (Costantini et al., 2021). EGMS is expected to have a wide range of users, including research institutes and universities; geological, geophysical, geodetic, and topographic surveys; civil protection authorities; public authorities (European, national, regional, and municipal levels); road and railway administrations; water management authorities; cultural heritage institutions; mining, oil, and gas industries; engineering firms; insurance firms; and citizens.

In this work we focus on the gradient of the deformation field. Analysing slope and aspect of the deformation field is the novelty of this investigation.

Most of the significant damages to manmade structures and infrastructures are associated with high deformation gradient values. Continuous monitoring for several years using satellite-based SAR data gives us the opportunity to calculate and analyse the deformation gradient in both rural and urban areas, including a large number of buildings.

This paper considers the local deformations that affect single structures or infrastructures. Local differences in such

deformation can indicate damages in the corresponding structure and infrastructure.

2. METHOD AND ANALYSIS

2.1 Data for Processing

Different types of products will be realized and provided by the EGMS:

- Level 2a (L2a): the Basic Product includes deformation velocity and deformation time series measured in both ascending and descending geometry. This product will be generated using the Sentinel-1 imagery at full resolution. Each frame will have an independent reference point for the deformation measurements. This product will be useful to carry out local deformation analyses.
- Level 2b (L2b): This represents a more advanced product, where the basic products will be calibrated using a GNSS reference network to provide products in a common reference frame, so that measurements are no longer relative to a reference MP.
- Level 3 (L3): These products offer a more advanced information, which comprises horizontal and vertical ground deformation, derived from multiple L2b products from complementary geometries. It will be provided in two geospatial layers: Vertical Up and Down and East-West components of displacement, both anchored to the GNSS reference network in a common reference frame. (Crosetto et al., 2020a), (Crosetto et al., 2020b).

In Spring 2022, the above products, generated using all S1 acquisitions from Feb. 2015 till Dec. 2020, will be made available via a dedicated EGMS portal. In this study we use a basic A-DInSAR product covering the municipality of Canillo (Andorra), which were generated at CTTC.

2.2 Study area

The “Forn de Canillo” area is located in the mountainous country of Andorra country, which is placed in the Central Pyrenees between Spain and France. The Canillo landslide is a challenge for geoscientist because of multiple smaller landslides near the village of Canillo.

2.3 Slope and aspect calculation

Studying land surface gradients, slope, and aspect, is possible using a digital elevation model. These parameters have been widely used in hydrological modelling, soil erosion investigations, and environmental simulations, etc (Zhou et al., 2004).

The novelty of this study is calculating the slope and aspect starting from a land displacement map. The local maximum deformation gradient (slope) is an essential parameter to be considered.

The slope identifies the steepness at each cell of a raster surface. The lower the slope value, the flatter the terrain; the higher the slope value, the steeper the terrain. Several algorithms have been developed to calculate slope. The simplest and most common is called the neighborhood method. The neighborhood method calculates the slope at one grid point by comparing the elevations of the eight grid points that surround it in 3 by 3 matrix. The neighborhood algorithm estimates the slope in the central cell by comparing the elevations of neighboring grid cells.

According to Eq.1, the neighborhood algorithm estimates percent slope at central grid cell (Z_5) as the sum of the absolute values of east-west slope and north-south slope to have a magnitude of slope value.

$$S_5 = \left(\sqrt{S^2_{e-w} + S^2_{n-s}}\right) \quad (1)$$

The aspect is the orientation of slope, measured clockwise in degrees from 0 to 360, where 0 is north-facing, 90 is east-facing, 180 is south-facing, and 270 is west-facing. An output aspect raster will typically result in several slope direction classes (Horn, B. K. P., 1981), (Austin et al., 2002).

2.4 Calculating slope and aspect with PS data

To monitoring anthropogenic and natural phenomena precisly and analyze the gradient deformation better in populated and rural areas, we presented an approach to separate PS data into two groups. One portion deal with PS points located within buildings, while the other one with PS points located outside of buildings and in rural areas.

We use for this operation OpenStreetMap data. OpenStreetMap is a free, editable map of the entire world that allows users to download urban coverage for majority of counties. As OpenStreetMap data are accessible in shapefile format in our study area, it was used to divide PS points. For this purpose, a tool was implemented with Python. To calculate differential deformation with slope values, we collected two groups of PS points as building and terrain data. The first step is to convert PS data from vector format to raster. This involves an interpolation. Inverse distance weighting (IDW) is commonly used to forecast unknown values for any vector data points (Setianto et at., 2013). IDW interpolation is deterministic method, which assumes that near values have a stronger relationship with the function than further values. IDW interpolation determines cell values using a linearly weighted combination of a set of sample points. The weight is a function of inverse distance. The surface being interpolated should be that of a locationally dependent variable. In this work, we considered a 7 by 7 m grid size for the IDW interpolation.

Finally, on the interpolated data, the slope and aspect are computed for both buildings and terrain data.

3. RESULT

As shown in Figure 2, in this study we focused on Canillo PS data which were derived from A-DInSAR techniques using SAR images from 2015-11-10 to 2021-02-14. The A-DInSAR processing generated Line-of-Sight (LOS) deformation time series and corresponding mean deformation velocity maps, which shows significant deformation rate, approximately -21 (mm/yr.), in south portion of Canillo.

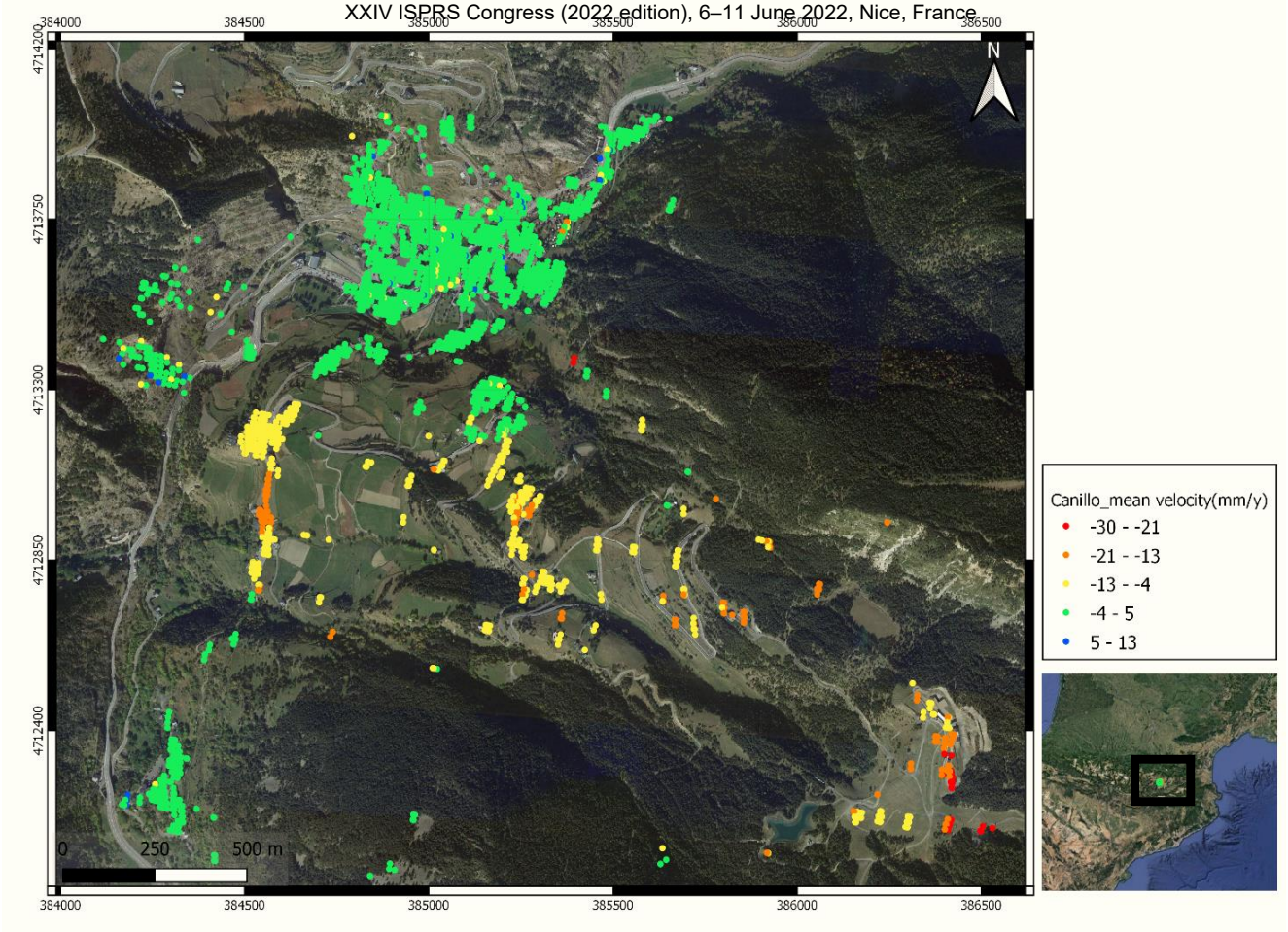

Figure 1. A plot of Mean velocity map in Canillo, in Andorra. Deformation velocity varies between -30 and 13 (mm/yr) from 2015 to 2021.

3.1 Terrain Differential Deformation Map

The first step of the procedure is to run the ADA-Finder software, which is a tool to identify Active Deformation Areas (ADA) from the A-DInSAR results. The ADA map is the main dataset to focus deeper analysis on the most significant moving areas, which have a potential impact in terms of risk. Active Deformation Area map has been generated using the ADA Finder tool, which makes a semi-automatic extraction from the A-DInSAR results of the most significant active areas, based on e methodology described in Barra et al., 2017. Each ADA polygon is a grouping of some adjacent points with a displacement velocity higher than a threshold. (For more information see Barra et al., 2017 and Barbier et al., 2021).

The ADA-Finder tool generates a buffer that includes all the neighbouring PS for every ADA. Points inside the ADA are active, while points inside the buffer are not. This is needed to perform a correct differential deformation analysis for terrain. In this study, seven ADA polygons were selected. Each polygons included more than seven PS points inside. The IDW interpolation and a Gaussian and Averaging filter were used to achieve smooth raster data.

Figures 2 and 3 show the Terrain Differential Deformation Map of the study area using Gaussian and Averaging filter, respectively. As it is shown in Figure 2, most of the parts in each polygon are green, which means there are no significant slopes, while in some parts there are slope variations in range between 0.5 to 1.1 (mm/yr/m). Also in Figure 3, Although most of the parts are green, few parts have slope values from 0.5 to 2 (mm/yr/m). We can infer high slope values in three ADA polygons based on slope values, indicating a high gradient in land deformation.

3.2 Building Differential Deformation Map

As mentioned before, to obtain the Building Differential Deformation Map, OpenStreetMap data for Andorra were used. All shapefile data related to buildings were downloaded and used for separating PS points.

IDW interpolation and Gaussian (sigma 2) filter were implemented again to related PS data to achieve a smooth raster data in urban area. Then we calculated slope and aspect to generate the Building Differential Deformation Map in the study area.

According to Figure 4, the Building Differential Deformation Map shows some significant gradient in urban area. This figure simply depicts the maximum value of each building's slope calculations. The slope values range from 0.0 to 0.6 (mm/yr/m), and the colour of polygons correspond to the building's maximum slope values (shown by the green triangle). Majority of buildings are green, safe, without any danger while six buildings, that were mentioned in Figure 4, have significant slope values in ranges between 0.1 to 0.3 (mm/yr/m). Black arrows also show the orientations of slope for each building. This map can indicate a problem for a given building: if one side of building has

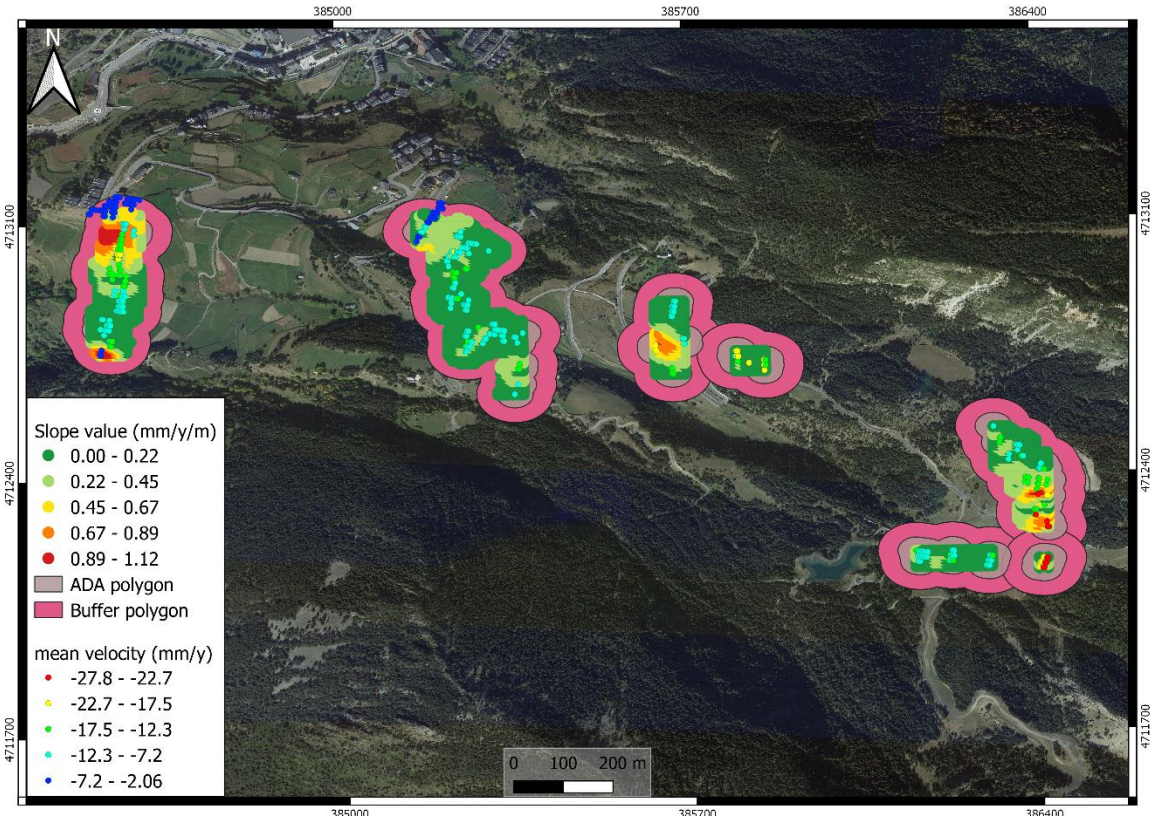

Figure 2. A Terrain Differential Deformation Map with Gaussian filter in rural areas. Slope values are from 0 to 1.12 (mm/yr/mm). Dark and light pink polygons show the Buffer and ADA polygons, respectively.

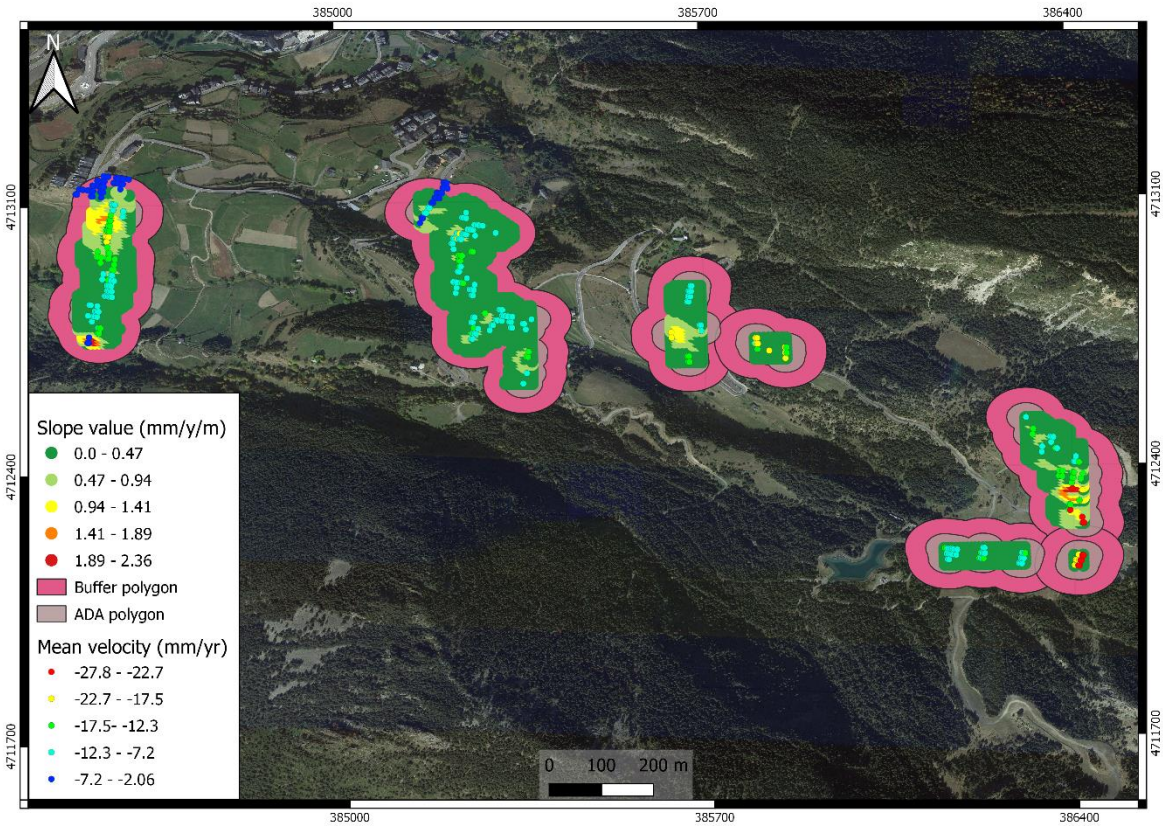

Figure 3. A Terrain Differential Deformation Map with Averaging filter in rural areas. Slope values are from 0 to 2.36 (mm/yr/mm). Dark and light pink polygons show the Buffer and ADA polygons, respectively.

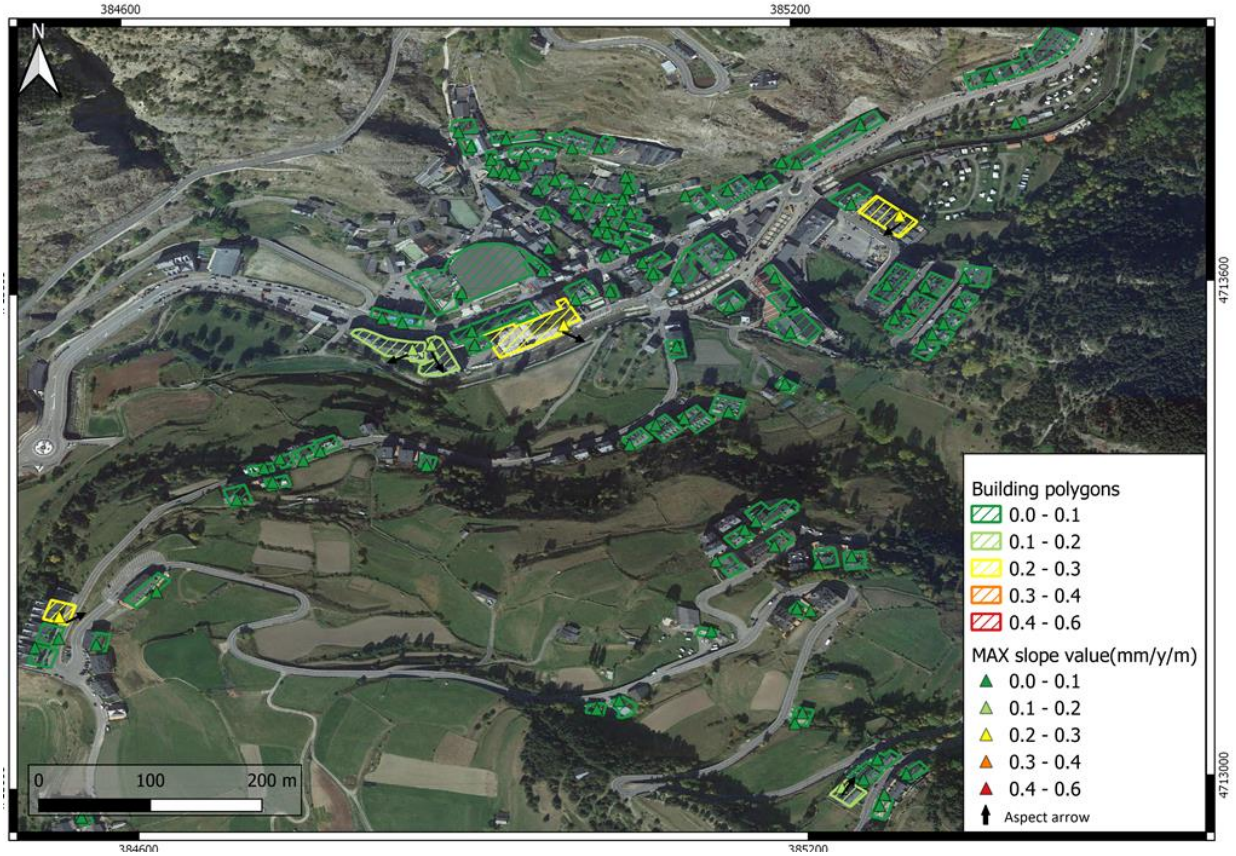

Figure 4. A Building Differential Deformation Map with Gaussian filter in the urban area of Canillo. Rectangles represent the polygon of buildings, and the color of polygons depends on the building's maximum slope value. six buildings have significant deformation slopes, whose black arrows show their deformation orientations.

deformation, but the opposite side does not have, some crack can appear on walls, etc. Consequently, monitoring the deformation variations and related gradients are effective in urban management and planning.

4. CONCLUSION

The gradient of the deformation fields measured by A-DInSAR is the focus of this study. This research calculates and analyses the range of slope and aspect of the land deformation field. EGMS products are designed for local and regional monitoring, and their resolutions are sufficient to explore at both levels. As a result, the local deformations that influence single structures or infrastructures are considered in this work.

Continuous monitoring for several years using satellite-based SAR data with millimeter precision gives us an opportunity to calculate and analyse the deformation gradient in both rural and urban areas. The ground displacement is derived from Synthetic Aperture Radar (SAR) time-series analysis of Sentinel-1A/B data. These data, which provide full coverage of Europe from two ascending and descending observation geometries every six days, are processed at full resolution.

In this work we use basic for A-DInSAR product which were generated at CTTC to have differential deformation map in the municipality of Canillo (Andorra).

In this work, we calculated slope and aspect for PS points inside and outside of buildings to obtain Building and Terrain Differential Deformation Maps, respectively. For Terrain differential deformation map using ADA finder tools were used to find active points and neighbourhood stable points. For Building differential deformation map, we used OpenStreetMap dataset which includes the polygons of buildings in shapefile format. In order to achieve such maps, PS data are transformed to a raster format by using the IDW interpolation method. The data are then filtered using an Averaging and Gaussian filter, to produce smooth deformation data. Calculating slope and aspect is the final step in creating Terrain and Building differential deformation maps in the study area.

The results achieved so far are encouraging. The future work will involve the study of wide areas, where the utility of the proposed product will be tested.

5. ACKNOWLEDGEMENTS

This work has been funded by the Agency for University and Research Grants Management, AGAUR, Generalitat de Catalunya, through a grant for the recruitment of early-stage research staff (Ref: 2021FI_B 00077).

This work is part of the Spanish Grant SARAI, PID2020-116540RB-C21, funded by MCIN/AEI/ 10.13039/501100011033.

6. REFERENCES

Austin, M. P. (2002). Spatial prediction of species distribution: an interface between ecological theory and statistical modelling. *Ecological modelling, 157*, 101–118.

Barra, A., Solari, L., Béjar-Pizarro, M., Monserrat, O., Bianchini, S., Herrera, G., . . . others. (2017). A methodology to detect and update active deformation areas based on sentinel-1 SAR images. *Remote sensing, 9*, 1002.

Costantini, M., Minati, F., Trillo, F., Ferretti, A., Novali, F., Passera, E., . . . others. (2021). European Ground Motion Service (EGMS). *2021 IEEE International Geoscience and Remote Sensing Symposium IGARSS*, (pp. 3293–3296).

Crosetto, M., Monserrat, O., Cuevas-González, M., Devanthéry, N., & Crippa, B. (2016). Persistent scatterer interferometry: A review. *ISPRS Journal of Photogrammetry and Remote Sensing, 115*, 78–89.

Crosetto, M., Solari, L., Balasis-Levinsen, J., Casagli, N., Frei, M., Oyen, A., & Moldestad, D. A. (2020a). Ground Deformation Monitoring At Continental Scale: The European Ground Motion Service. *International Archives of the Photogrammetry, Remote Sensing & Spatial Information Sciences, 43*.

Crosetto, M., Solari, L., Mróz, M., Balasis-Levinsen, J., Casagli, N., Frei, M., et al. (2020b). The evolution of wide-area DInSAR: From regional and national services to the European Ground Motion Service. *Remote Sensing, 12*, 2043.

Ferretti, A., Prati, C., & Rocca, F. (2000). Nonlinear subsidence rate estimation using permanent scatterers in differential SAR interferometry. *IEEE Transactions on geoscience and remote sensing, 38*, 2202–2212.

Ferretti, A., Prati, C., & Rocca, F. (2001). Permanent scatterers in SAR interferometry. *IEEE Transactions on geoscience and remote sensing, 39*, 8–20.

Gasc-Barbier, M., Barra, A., Buxó, P., Trapero, L., Crosetto, M., Colell, X., . . . Marturia, J. (2021). Monitoring deformations related to geological risks with InSaR data–the MOMPA project. *IOP Conference Series: Earth and Environmental Science, 833*, p. 012142.

Horn, B. K. (1981). Hill shading and the reflectance map. *Proceedings of the IEEE, 69*, 14–47.

Setianto, A., & Triandini, T. (2013). Comparison of kriging and inverse distance weighted (IDW) interpolation methods in lineament extraction and analysis. *Journal of Applied Geology, 5*.

Zhou, Q., & Liu, X. (2004). Analysis of errors of derived slope and aspect related to DEM data properties. *Computers & Geosciences, 30*, 369–378.